Dictionary-learning compressed-sensing reconstruction with anisotropic density-adapted radial acquisition for sodium quantification using ^{23}Na-MRI

Matthias Utzschneider[1,3], Nicolas G.R. Behl[2], Sebastian Lachner[1], Lena V. Gast[1] , Andreas Maier[3,4], Michael Uder[1], Armin M. Nagel[1,2]

[1]Institute of Radiology, University Hospital Erlangen, Friedrich-Alexander-Universität Erlangen-Nürnberg (FAU), Erlangen, Germany, [2]Division of Medical Physics in Radiology, German Cancer Research Centre (DKFZ), Heidelberg, Germany, [3]Pattern Recognition Lab, Friedrich-Alexander-Universität Erlangen-Nürnberg (FAU), Erlangen, Germany [4]Erlangen Graduate School in Advanced Optical Technologies, Erlangen, Germany

Target Audience: Clinicians and scientist involved in musculoskeletal applications of sodium MRI.

Purpose

Sodium MRI (^{23}Na-MRI) has great potential for the examination of musculoskeletal diseases[1]. Accurate quantification of ^{23}Na in different tissue types is important for these applications and is a general research topic[2]. However, ^{23}Na-MRI suffers from poor signal-to-noise ratio due to low MR sensitivity of ^{23}Na and low in-vivo concentration. Anisotropic acquisition techniques can improve the in-plane resolution for elongated structures like muscle tissue; e.g. a density-adapted radial acquisition scheme can be used to sample a cuboid[3] (DA-3DPR-C). Sparsity-based reconstruction techniques such as compressed sensing[4] (CS) can be employed to improve image quality in ^{23}Na-MRI. In this study, the Dictionary-Learning Compressed Sensing[5] (DLCS) reconstruction algorithm is applied to highly undersampled data. Both, simulations and in-vivo measurements were performed to analyze the ^{23}Na-quantification error in muscle tissue.

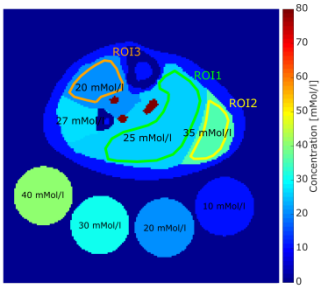

Figure 1: Simulated Phantom with assigned sodium concentrations and ROIs.

Methods

^{23}Na-MRI was conducted on a 3-T whole body system (Magnetom 3-T Skyra, Siemens Healthineers Erlangen, Germany). Fully- and undersampled data sets were acquired and simulated. The spatial resolution of all images is 3x3x15mm^3. Simulation study: An analytical phantom of the human calf was created based on high-resolution ^{1}H-MRI data including four reference tubes containing NaCl solution (10, 20, 30, 40 mM). Different sodium concentrations were assigned to the tissue types corresponding to research[2] (fat tissue: 10 mM, blood vessels: 80 mM, muscle tissue: 20-35 mM, see Figure 1). Simulation parameters were chosen to match the in-vivo study (see next subsection). White Gaussian noise was added to match the noise level of the measurements. In-vivo study: ^{23}Na-MR images were acquired of the right calf muscle of one healthy female volunteer (61 yrs. old). Four tubes with NaCl (10, 20, 30, 40 mM) were placed inside the receiver coil below the calf for quantification. In the following, the distribution of projection endpoints on the sampled cuboid[3], the undersampling factor (USF) and acquisition time (TA) are shown in brackets with the projection number. A fully sampled data set with 9080 projections (52x52x20, USF: 1, TA: 22m42s) was acquired for reference. Undersampled data sets with 3152 (26x26x20, USF: 2.9, TA: 7m53s), 2168 (20x20x20, USF: 4.2, TA: 5m25s) and 1352 (16x16x16, USF: 6.7, TA: 3m23s) projections were measured without averaging. Acquisition parameters: TE/ TR = 0.30/150 ms; α = 90°; readout duration TRO = 5 ms. Reconstruction: The iterative DLCS algorithm is used to reconstruct images from the undersampled data sets (Parameters: block-size: 3^3, dictionary size: 800). For comparison, conventional reconstruction is performed consisting of a regridding of the radially acquired raw data and a fast Fourier Transform (rFFT). A Hamming filter is applied to the raw data prior to the conventional reconstruction to reduce Gibb's ringing artifacts and to improve SNR. Quantification method: For quantification, linear interpolation of the signal intensities of the reference tubes was used. Regions of Interests (ROIs) were defined (see Figure 2). Mean concentration and standard deviation (SD) are computed for these ROIs.

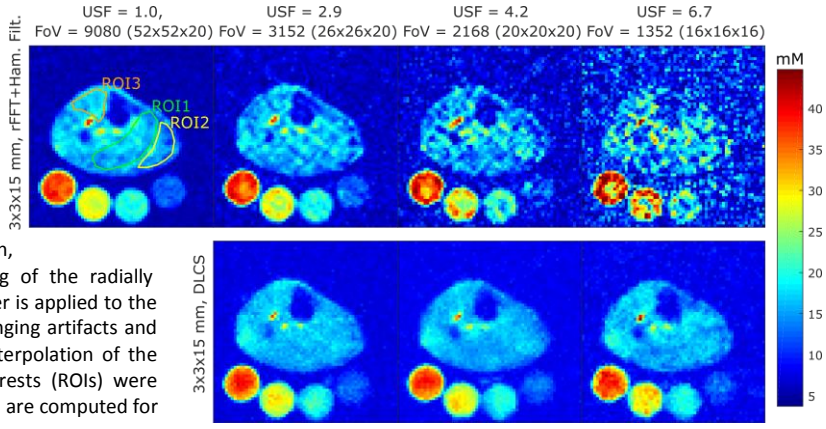

Figure 2: In-vivo ^{23}Na images of a calf with reference tubes and quantification ROIs.

Results

The mean concentrations of the simulated phantom are reconstructed with DLCS for USF: 2.9 and USF: 4.7 with a maximum deviation of 4% from the ground truth (GT). The SD is significantly reduced (DLCS: ± 2 to ± 3.2 mM) compared to the rFFT with Hamming filter (rFFT: ± 3.9 to ± 8.1 mM). For higher USFs DLCS yields a maximum deviation of 8% from GT (SD: 1.6 to 2.7, see Table 1). The in-vivo concentrations in images reconstructed with DLCS (see Figure 2) match the values of a fully sampled image with a maximum deviation of 8% and the SD is overall lower for DLCS (± 1.3 to ± 2.0 mM) compared to the rFFT (± 2.7 to ± 7.5 mM).

Discussion and Conclusion

The application of DLCS to undersampled ^{23}Na-MRI data acquired with DA-3DPR-C yields great potential to reduce measurement time for ^{23}Na-quantification while preserving a high accuracy.

Table 1: Observed concentrations for simulated data sets. Values for DLCS are indicated for USF>1 and values for rFFT for same USFs shown in brackets.

mM	ROI1	ROI2	ROI3
GT	25	35	20
rFFT,USF: 1	24.6 ± 1.7	35.3 ± 2.5	18.9 ± 2.2
DLCS, USF: 2.9	25.5 ± 2.2	34.9 ± 2	20.2 ± 2.6
rFFT, USF: 2.9	(25.1 ± 4.5)	(34.5 ± 3.9)	(19.4 ± 4.1)
DLCS, USF: 4.7	26 ± 2.7	34.4 ± 2.6	20.5 ± 3.2
rFFT, USF: 4.7	(24.9 ± 7.5)	(35.6 ± 8.1)	(18.0 ± 5.8)
DLCS, USF: 6.7	25.6 ± 2.7	32.5 ± 2.7	20.1 ± 1.6
rFFT, USF: 6.7	(22 ± 11.5)	(35.5 ± 11.3)	(14.4 ± 11.8)

Table 2: Observed concentrations for in-vivo measurements. Values for DLCS are indicated for USF>1 and values for rFFT for same USFs shown in brackets.

mM	ROI1	ROI2	ROI3
rFFT,USF: 1	15.4 ± 2.4	13.1 ± 2.9	16.7 ± 1.9
DLCS, USF: 2.9	14.4 ± 1.5	13.7 ± 1.9	15.3 ± 1.5
rFFT, USF: 2.9	(14.9 ± 3.2)	(13.2 ± 3.9)	(15 ± 2.7)
DLCS, USF: 4.7	14.6 ± 1.2	14.1 ± 1.9	15.6 ± 1.2
rFFT, USF: 4.7	(14.6 ± 4.2)	(13.6 ± 5.6)	(14.9 ± 4.6)
DLCS, USF: 6.7	14.8 ± 1.9	14.2 ± 2	16 ± 1.4
rFFT, USF: 6.7	(16.3 ± 6.7)	(14.8 ± 7.5)	(16.4 ± 6.5)

References

1. Nagel AM, Weber MA et al. (2013) Skeletal Muscle MR Imaging Beyond Protons: With a Focus on Sodium MRI in Musculoskeletal Applications. MRI Skl Musc: pp. 115-133.
2. Constantinides CD, Gillen JS, et al., Human Skeletal Muscle: Sodium MR Imaging and Quantification – Potential Applications in Exercise and Disease. Rad 2000; 216(2): pp. 559-68.
3. Nagel AM et al. (2012): 3D Density-Adapted Projection Reconstruction 23Na-MRI with Anisotropic Resolution and Field-of-View. Proc Intl Soc Mag Reson. (2012): pp. 674. 4.
4. Lustig M, Donoho D, et al. Sparse MRI (2007): The Application of Compressed Sensing for Rapid MR Imaging. Magn Reson Med. 2007; 58(6): pp. 1182-95. 5.
5. Behl NGR, Gnahm C, et al. (2016) Three-Dimensional Dictionary-Learning Reconstruction of 23Na MRI Data. Magn Reson Med. 2016; 75: pp. 1605-16.